

Original Article

Hippocampus avoidance with fan beam and volumetric arc radiotherapy for base of skull tumours

Ericka Wiebe¹, Luca Cozzi⁶, Slav Yartsev^{2–4}, Antonella Fogliata⁶, Alessandro Clivio⁶, Eugenio Vanetti⁶, Giorgia Nicolini⁶, Jeff Chen^{2–4}, Andrew Leung⁵, Glenn Bauman^{1,3,4}

¹Department of Radiation Oncology, ²Department of Physics and Engineering, London Regional Cancer Program, ³Department of Medical Biophysics, ⁴Department of Oncology, ⁵Department of Medical Imaging, London Health Sciences Centre and Schulich School of Medicine & Dentistry, University of Western Ontario, Canada, ⁶Medical Physics Unit, Oncology Institute of Southern Switzerland, Bellinzona, Switzerland

Abstract

Radiosensitive neurogenic stem cells reside in the hippocampi, suggesting that avoidance of the hippocampi may be an important strategy to reduce potential radiation-related cognitive effects. Six patients treated for base of skull tumours were re-planned using co-planar helical fan beam arc therapy (tomotherapy) and co-planar and non-coplanar volumetric arc techniques (RapidArc). The hippocampi were contoured as avoidance structures with the specific goal of minimising the dose. Two gross target volume (GTV) to planning target volume (PTV) expansions (10 and 2 mm) were considered to evaluate the impact of margin selection on organ at risk (OAR) sparing. The dose prescription was 50 Gy to >95% of the PTV. Comparison of the hippocampus avoidance plans demonstrated the importance of non-coplanar delivery when the 10 mm margin was used. With the 2 mm margin, both co-planar and non-coplanar delivery provided similar degrees of sparing. A mean dose of 3–4 Gy and a $V_{6Gy} < 5\%$ to the hippocampi was realised with the hippocampus sparing techniques. Our comparisons suggest interventions to minimise GTV to PTV margins will have a more profound influence on multiple OAR sparing than the choice of intensity modulated arc delivery technique.

Keywords

Hippocampus; intensity modulated radiotherapy; brain tumour

INTRODUCTION

Late radiation toxicity of the central nervous system (CNS) tissue generally becomes evident 6 months or later after irradiation. These side effects are generally irreversible and progressive, and may manifest as focal brain injury or

cognitive impairment. Specifically, memory impairment and neurocognitive dysfunction can be treatment-related morbidities which are particularly problematic in patients with extended survival.¹ Patients with benign base of brain tumours, such as meningioma and pituitary adenoma, tend to have high rates of local control after radiation. Given the associated long survival, these patients are at risk for neurocognitive late effects.^{2–4} The typical growth pattern of these tumours is expansile

Correspondence to: Glenn Bauman, Department of Radiation Oncology, London Regional Cancer Program, Department of Medical Imaging, London Health Sciences Centre, 790 Commissioners Rd E, London, Ontario, N6A 4L6, Canada. Email: glenn.bauman@lhsc.on.ca

and minimally invasive, providing an opportunity to minimise late side effects through advanced radiotherapy delivery techniques⁵ that avoid critical structures and minimise the volume of brain irradiated.

Radiation injury of the brain is mediated by many different pathways including small vessel injury, inflammatory effects and demyelination. The effect of radiation on neurogenic stem cells is also a possible contributor to late cognitive effects. Specifically, radiation-induced impairment of neurogenesis in the subventricular zone of the lateral ventricles and the subgranular zone of the dentate gyrus of the hippocampus has been identified as a potential mediator of late effects contributing to neurocognitive dysfunction.⁶ Recognition that neurogenesis occurs in the hippocampus of adult humans⁷ suggests that radiation injury to this structure could have significant implications for neurocognitive function. Similar to other populations of stem cells, neural stem cells in the hippocampus are highly sensitive to radiation.^{6,8}

Advanced radiation planning techniques have been proposed to decrease the neurocognitive morbidity by decreasing dose to the medial temporal lobe where the hippocampi are located.^{8–11} Focal radiotherapy for base of skull lesions with proximity of the medial temporal lobes to base of skull structures also puts the hippocampi at risk and they are particularly subjected to moderately high radiation doses in traditional two- or three-field techniques that incorporate lateral beam arrangements.¹² The conformal avoidance properties of helical tomotherapy (HT) have been previously demonstrated to provide a favourable balance of planning target volume (PTV) coverage, conformal dose, and organ at risk sparing compared to other radiotherapy techniques for base of skull tumours using non-hippocampus sparing techniques.¹³ Our primary goals with this comparative study were to (i) identify the magnitude of hippocampus sparing that might be achievable with various intensity-modulated arc techniques and PTVs, and (ii) delineate the importance of non-coplanar versus coplanar techniques to realise this benefit.

MATERIALS AND METHODS

Six patients with base of brain tumours (four pituitary adenoma, two meningioma of the parasellar region) previously treated at the London Regional Cancer Program were selected for this planning study. All patients had been previously scanned using a helical CT scanner (Philips 5000) with 3 mm slice thickness from the vertex of the skull to the bottom of the second thoracic vertebral body.

Hippocampus contours were defined with reference to previous protocols for delineating hippocampus volumes on MRI¹⁴ and input from an experienced neuro-radiologist (A.L.). A set of anatomic boundaries was developed to delineate the hippocampus on axial CT images. The anterior boundary was defined by the most anterior aspect of the temporal horn. The lateral boundary was the medial wall of the temporal horn. The medial margin was the cerebral spinal fluid in the uncus and ambient cisterns. The posterior extent was defined by a line between the atrium of the lateral ventricle and the colliculi. Superiorly, the hippocampi were contoured to the level of the superior colliculi. The inferior boundary was at the level of the interpeduncular cistern and dorsum sellae. The hippocampi were contoured by the same individual (E.W.), based on CT data and, where available (two sets), were cross-referenced with MRI data.

Organs at risk (OARs) were otherwise delineated as for the initial treatment plan. Avoidance structures contoured include lens, eyes, optic nerves, cerebrum, cerebellum, and brainstem. Maximum OAR doses were defined as: brain, brain stem, optic chiasm, and optic nerves: 50 Gy; eye (whole): 20 Gy; lens with 3 mm margin: 7 Gy. PTVs using margins of 10 mm (PTV10) and 2 mm (PTV2) were defined based on the previously delineated gross tumour [gross target volume (GTV)] used for clinical treatment. The 10 mm margin included a 5 mm clinical target volume (CTV) expansion and an additional 5 mm PTV expansion which reflects current uncertainty in target volume delineation on CT and immobilisation with our mask-based

immobilisation. The PTV2 scenario was explored to approximate the degree of hippocampus sparing that might be achieved with the use of multi-modality target volume delineation and image guidance technologies. In all plans, the prescription dose for this study was 50 Gy in 25 fractions, with 95% of the PTV to receive at least 50 Gy.

Tomotherapy treatment planning

CT datasets and structures were transferred to the tomotherapy planning workstation (TomoTherapy Inc., Madison, Wisconsin) using the DICOM RT protocol. The tomotherapy station re-sampled the CT datasets in 256×256 voxels with slice thickness re-sampled to the smallest slice separation in the original CT data-set. The planning system used an inverse treatment planning process based on iterative least squares minimisation of an objective function.¹⁵ A superposition/convolution algorithm was used to calculate the dose. The optimisation was guided using precedence, importance, and penalty factor parameters for CNS as previously described,¹⁶ with the addition of the hippocampus as an avoidance structure. HT optimisation parameters included fan field width of 2.5 cm, pitch of 0.215, and a modulation factor of 3.0. Tomotherapy plans were generated for PTV10 and PTV2 options that sought to achieve maximum hippocampus sparing while maintaining PTV coverage and irradiation to other OAR at or below the defined tolerance limits.

Volumetric arc treatment planning

RapidArc uses continuous variation of the instantaneous dose rate, MLC leaf positions, and gantry rotational speed to optimise the dose distribution. Details of the RapidArc optimisation process have been published previously by our group.^{17,18} To minimise the contribution of tongue and groove effect during the arc rotation, as well as to benefit from leaf trajectories non-coplanar with respect to patient's axis, the collimator rotation in RapidArc remains fixed to a non-zero value. In the present study, the collimator was rotated to 40° . For the volumetric arc treatment plan-

ning, three plans for each of PTV10 and PTV2 were generated: rapid arc (RA)_1, a single coplanar arc 360° long; RA_2, one coplanar arc (360°) and one orthogonal arc of 180° from (180° to 0°) with couch angles of 0° and 90° , respectively; RA_3, one coplanar arc 360° long and two non-coplanar arcs 210° long from 180° to 30° with couch angles of 0° , -45° and $+45^\circ$, respectively. As for the HT plans, the RA plans were designed for maximum hippocampus sparing while maintaining PTV coverage and while keeping other OAR doses at or below the defined tolerance limits.

Plan comparison metrics

For PTV coverage, DVH parameters of D_{99} , D_{95} , and D_1 were used for comparison purposes. D_{99} and D_1 were used as substitutes for minimum and maximum dose, respectively, to avoid erroneous comparison of dose per voxel metrics for different calculation grids in HT and RA treatment planning systems. For brain (PTV excluded), D_5 , D_{20} , and D_{50} ; and for brainstem, D_1 , D_{10} , and D_{50} were the primary metrics for comparison. Relevant clinical parameters remain speculative for hippocampi comparisons. For sparing directed at the stem cell population which is quite radiosensitive, volume based parameters reflecting dose to the entire structure (i.e., mean dose) are important and this was therefore included as a comparison metric. Recognising the exquisite radiosensitivity of stem cell populations, Gutiérrez et al. set objectives of keeping the dose to the entire hippocampi less than 6 Gy.¹¹ Other authors have noted a threshold for neurocognitive side effects and MRI changes when doses exceed 18–20 Gy.¹⁹ Thus dose metrics of D_5 , D_{20} , D_{50} , V_{6Gy} , and V_{18Gy} to both unilateral hippocampi and as a paired structure were analyzed. We also examined metrics for OARs including eyes and optic nerves. Cumulative dose–volume histograms for the six patients for the GTV, PTV and OAR were calculated. Differences in dose–volume outcomes of the treatment planning parameters were assessed for significance using paired, two-sided *t*-tests with significance of the *p* value set at <0.01 to adjust for multiple comparisons.

RESULTS

An illustration of a non-hippocampus sparing versus hippocampus sparing HT plan for a patient with a pituitary tumour is illustrated in Figure 1. In delineating the hippocampus as avoidance structures for our series of six patients, the total hippocampus volumes contoured ranged from 8.52 to 11.23 cm³, in comparison to literature values of total hippocampus volumes of 4.99 cm³ (ref. 11) to 5.66 cm³ (ref. 20). Our volumes may have been somewhat larger due to the lower resolution of the hippocampus on CT imaging required a contouring approach delineated by anatomical boundaries with greater inherent margin than MRI-based planning.

A comparison among the hippocampus sparing techniques including target volume coverage, hippocampus sparing and other OAR sparing is outlined in Tables 1 and 2 for the 10 and 2 mm margin plans, respectively. Examination of the raw data demonstrated no difference in results between hippocampi as separate structures versus as a single structure, thus the table includes the results for the hippocampi as a combined structure. An illustration of the coplanar and non-coplanar plans hippocampus sparing plans is shown in Figure 2. Composite dose–volume histograms for the six patients planned are presented in Figure 3.

Inspection of the results revealed that the maximum hippocampus sparing was achieved with the combination of the 2 mm PTV margin and a three non-coplanar arc plan, i.e., RA2_3, where the V_{6Gy} and V_{18Gy} were <5% and 0%, respectively, and the average mean dose was 3 ± 0.3 Gy (Figure 2b and Table 2). However, with a 2 mm PTV margin, all techniques (coplanar or non-coplanar) conferred significant hippocampus sparing. Comparisons of dose delivered to other OAR (brain, brainstem, optic nerves) revealed differences between the five techniques; although these differences were generally small and of a magnitude that is unlikely to be clinically important. In addition, no attempt was made to minimise dose to non-hippocampus OAR provided the tolerance thresholds were respected. The non-coplanar techniques were not associated with a meaningfully higher integral dose or mean dose to brain compared to coplanar techniques.

More pronounced differences between the different techniques were seen with the use of the larger, 10 mm PTV margins. In particular, for the most stringent hippocampus parameter (V_{6Gy}), only the non-coplanar plans were able to provide meaningful sparing with approximately 50% of the hippocampus volume maintained below 6 Gy. The PTV10 HT plans

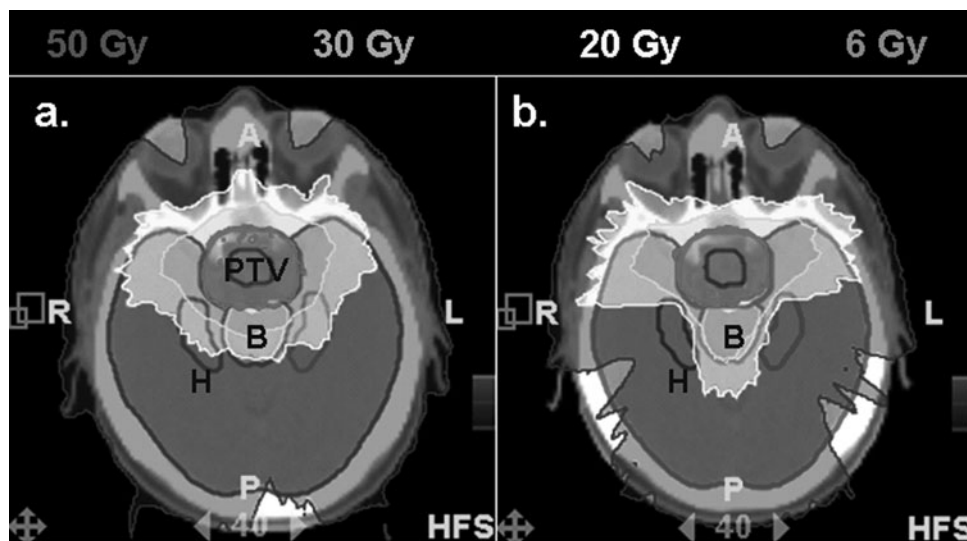


Figure 1. A non-hippocampus sparing HT plan (left) compared to a maximally sparing HT plan (right). Significant hippocampus (H) sparing is achieved but at the expense of slightly higher brainstem (B) dose and heterogeneity of dose in the PTV.

Table 1. Comparisons using a 10mm PTV margin (PTV10)

Organ/Structure	Parameter	HT10	RA10_1	RA10_2	RA10_3	<i>p</i> < 0.05
GTV	Mean (Gy)	50.7 ± 0.2	50.8 ± 0.3	50.6 ± 0.2	50.5 ± 0.2	e
	D1% (Gy)	51.4 ± 0.5	51.6 ± 0.3	51.1 ± 0.3	51.1 ± 0.2	e
	D5% (Gy)	51.2 ± 0.4	51.3 ± 0.3	51.0 ± 0.3	50.9 ± 0.2	e
	D95% (Gy)	50.3 ± 0.1	50.3 ± 0.4	50.3 ± 0.2	50.2 ± 0.2	
	D99% (Gy)	50.1 ± 0.1	50.1 ± 0.3	50.1 ± 0.2	50.0 ± 0.3	
	V95% (%)	100.0 ± 0.0	100.0 ± 0.0	100.0 ± 0.0	100.0 ± 0.0	
PTV10	Mean (Gy)	50.7 ± 0.2	51.0 ± 0.2	50.8 ± 0.2	50.8 ± 0.2	a,e
	D1% (Gy)	51.5 ± 0.4	52.6 ± 0.3	52.1 ± 0.3	52.0 ± 0.3	a,b,c,d,e
	D5% (Gy)	51.2 ± 0.3	52.1 ± 0.3	51.7 ± 0.2	51.7 ± 0.2	a,b,c,e
	D95% (Gy)	50.0 ± 0.0	50.0 ± 0.0	50.0 ± 0.0	50.0 ± 0.0	
	D99% (Gy)	48.6 ± 1.4	49.3 ± 0.3	49.2 ± 0.3	49.2 ± 0.3	
	V95% (%)	99.6 ± 0.6	99.8 ± 0.2	99.9 ± 0.1	99.9 ± 0.2	
	Brain	Mean (Gy)	11.6 ± 2.1	7.3 ± 2.4	8.0 ± 2.0	8.0 ± 1.9
D5% (Gy)		37.0 ± 6.4	30.9 ± 8.2	26.2 ± 9.3	26.5 ± 9.4	a,b,c,d,e
D20% (Gy)		17.8 ± 2.7	12.4 ± 3.9	12.0 ± 2.8	11.6 ± 2.4	a,b,c
D50% (Gy)		9.0 ± 1.8	2.5 ± 2.7	5.4 ± 1.4	5.5 ± 1.3	a,b,c,d,e
V10Gy (%)		46.0 ± 8.7	25.7 ± 9.3	25.9 ± 7.6	24.9 ± 7.0	a,b,c
CI95%		1.6 ± 0.3	1.4 ± 0.2	1.4 ± 0.3	1.4 ± 0.2	b,c
EI (%)		37.4 ± 25.9	32.8 ± 21.6	29.5 ± 23.1	29.6 ± 22.0	
ID		1.50 ± 3.46	0.96 ± 3.62	1.03 ± 3.14	1.04 ± 3.05	a,b,c,e
Brainstem	Mean (Gy)	32.0 ± 2.9	26.4 ± 1.7	24.1 ± 3.0	23.7 ± 2.7	a,b,c,d,e
	D1% (Gy)	50.7 ± 0.5	50.8 ± 0.5	50.1 ± 0.8	50.5 ± 0.7	b,d,f
	D10% (Gy)	47.7 ± 2.1	47.1 ± 2.6	43.8 ± 6.0	44.8 ± 4.7	c,e
	D50% (Gy)	32.1 ± 3.3	28.5 ± 3.1	21.9 ± 3.0	22.5 ± 2.8	b,c,d,e
Hippocampus	Mean (Gy)	15.3 ± 1.1	11.3 ± 1.3	7.4 ± 1.2	7.2 ± 0.9	a,b,c,d,e
	D1% (Gy)	25.2 ± 2.7	21.0 ± 3.5	20.1 ± 5.7	19.6 ± 5.1	
	D5% (Gy)	20.8 ± 1.2	16.9 ± 1.9	14.4 ± 3.5	13.9 ± 3.1	a,b,c,d,e
	D20% (Gy)	17.4 ± 0.6	13.5 ± 1.4	9.7 ± 1.7	9.3 ± 1.3	a,b,c,d,e
	D50% (Gy)	14.9 ± 0.9	10.7 ± 1.2	6.5 ± 1.0	6.3 ± 0.5	a,b,c,d,e
	V6Gy (%)	100.0 ± 0.0	98.1 ± 3.0	55.7 ± 12.2	54.4 ± 7.8	b,c,d,e
	V18Gy (%)	15.7 ± 4.5	3.7 ± 3.1	2.3 ± 2.4	2.0 ± 2.1	a,b,c,d,e
L Optic Nerve	Mean (Gy)	26.6 ± 6.8	25.5 ± 9.2	19.7 ± 9.3	19.1 ± 8.9	b,c,d,e
	D1% (Gy)	43.2 ± 9.3	40.7 ± 11.6	38.4 ± 14.4	37.8 ± 15.0	
	D10% (Gy)	38.5 ± 12.6	37.0 ± 14.3	34.4 ± 16.7	33.6 ± 17.1	d
	D50% (Gy)	25.2 ± 7.5	24.1 ± 10.0	17.9 ± 11.5	16.9 ± 9.6	b,c,d,e
R Optic Nerve	Mean (Gy)	27.4 ± 5.5	25.8 ± 7.6	17.7 ± 7.6	17.5 ± 6.6	b,c,d,e
	D1% (Gy)	47.8 ± 4.5	46.4 ± 7.6	42.9 ± 12.6	43.0 ± 12.1	
	D10% (Gy)	42.6 ± 9.9	40.2 ± 12.1	36.3 ± 16.4	36.0 ± 16.2	
	D50% (Gy)	24.9 ± 6.1	22.9 ± 7.0	12.8 ± 6.3	12.5 ± 4.5	b,c,d,e
Lens	D1% (Gy)	5.5 ± 1.5	6.6 ± 2.0	2.6 ± 0.9	2.7 ± 1.1	b,c,d,e

p < 0.05: comparisons significant at a level of 0.05 or less; CI95%: conformity index for 95% isodoses. EI%: percentage of brain receiving more than prescription dose; ID: Integral dose ($10^5 \times \text{Gy} \times \text{cm}^3$)

Comparisons: a: HT10 vs. RA10_1; b: HT10 vs. RA10_2; c: HT10 vs. RA10_3; d: RA10_1 vs. RA10_2; e: RA10_1 vs. RA10_3; f: RA10_2 vs. RA10_3; i.e., RA10_1 vs. RA10_3 is RA plan with 10mm PTV, 1 co-planar arc compared to RA plan with 10mm PTV and 3 non-coplanar fields.

provided the least hippocampus sparing and less brain sparing (Table 1). Larger doses to the tissue just above and below the target in HT plans (see right hand panels in Figures 2a,b coronal and sagittal views) are due to the helical delivery with fixed fan beam width. This effect could be eliminated with the implementation of a moving jaw.^{21,22} Comparison of other OAR doses

revealed less favourable dose metrics with the larger PTV margin, and less advantage with non-coplanar techniques compared to the coplanar techniques.

With respect to the tumour coverage, the introduction of hippocampus sparing was achieved without compromising target

Table 2. Comparisons using a 2mm PTV margin (PTV2)

Organ/Structure	Parameter	HT2	RA2_1	RA2_2	RA2_3	p < 0.05
GTV	Mean (Gy)	51.4 ± 0.1	50.9 ± 0.3	50.6 ± 0.3	50.7 ± 0.4	a,b,c
	D1% (Gy)	52.5 ± 0.4	51.5 ± 0.3	51.3 ± 0.3	51.3 ± 0.5	a,b,c
	D5% (Gy)	52.2 ± 0.4	51.3 ± 0.3	51.1 ± 0.3	51.1 ± 0.5	a,b,c
	D95% (Gy)	50.3 ± 0.1	50.4 ± 0.3	50.3 ± 0.4	50.4 ± 0.4	
	D99% (Gy)	49.8 ± 0.1	50.2 ± 0.2	50.1 ± 0.4	50.3 ± 0.4	a
	V95% (%)	100.0 ± 0.0	100.0 ± 0.0	100.0 ± 0.0	100.0 ± 0.0	
PTV2	Mean (Gy)	51.3 ± 0.2	50.8 ± 0.2	50.7 ± 0.2	50.7 ± 0.3	a,b,c
	D1% (Gy)	52.6 ± 0.4	51.8 ± 0.4	51.6 ± 0.2	51.6 ± 0.4	a,b,c
	D5% (Gy)	52.3 ± 0.4	51.5 ± 0.4	51.4 ± 0.2	51.4 ± 0.4	a,b,c
	D95% (Gy)	50.0 ± 0.0	50.0 ± 0.0	50.0 ± 0.0	50.0 ± 0.0	
	D99% (Gy)	48.2 ± 0.5	49.0 ± 0.4	49.4 ± 0.2	49.4 ± 0.2	a,b,c
	V95% (%)	99.5 ± 0.4	99.9 ± 0.1	100.0 ± 0.0	100.0 ± 0.0	a,b,c
Brain	Mean (Gy)	5.9 ± 1.7	4.1 ± 1.7	4.5 ± 1.4	4.3 ± 1.4	a,b,c,f
	D5% (Gy)	25.7 ± 5.1	19.5 ± 6.2	14.4 ± 4.6	14.0 ± 5.4	a,b,c,d,e
	D20% (Gy)	9.7 ± 3.7	6.3 ± 3.0	7.5 ± 1.8	6.6 ± 1.6	a,c,f
	D50% (Gy)	1.9 ± 1.2	0.9 ± 0.8	2.6 ± 1.0	2.6 ± 0.9	a,c,d,e
	V10Gy (%)	19.4 ± 6.1	12.7 ± 5.5	11.5 ± 6.1	9.1 ± 4.8	a,b,c,e,f
	CI95%	1.5 ± 0.5	1.3 ± 0.4	1.3 ± 0.4	1.3 ± 0.4	b,c
	EI (%)	28.0 ± 36.5	23.4 ± 33.0	21.8 ± 31.0	21.6 ± 31.3	
	ID	7.76 ± 2.56	5.36 ± 2.54	5.912 ± 2.167	5.66 ± 2.19	a,b,c,f
Brainstem	Mean (Gy)	19.0 ± 5.0	15.6 ± 2.2	14.1 ± 1.8	12.9 ± 1.8	a,b,c,e,f
	D1% (Gy)	41.0 ± 7.8	40.9 ± 5.6	37.6 ± 7.4	37.8 ± 7.4	b,d,e,f
	D10% (Gy)	31.8 ± 6.9	31.3 ± 3.1	24.8 ± 3.8	24.5 ± 4.3	b,c,d,e
	D50% (Gy)	19.7 ± 6.7	15.2 ± 3.4	12.9 ± 1.9	12.3 ± 1.8	b,c,e,f
Hippocampus	Mean (Gy)	4.1 ± 0.5	4.2 ± 0.9	3.0 ± 0.4	3.0 ± 0.3	b,c,d,e
	D1% (Gy)	20.6 ± 3.3	14.0 ± 5.0	8.4 ± 1.8	8.3 ± 1.5	a,b,c,d,e
	D5% (Gy)	13.6 ± 3.8	9.6 ± 2.9	5.9 ± 1.5	5.9 ± 1.1	a,b,c,d,e
	D20% (Gy)	3.9 ± 0.3	5.1 ± 1.0	3.7 ± 0.6	3.7 ± 0.4	a,d,e
	D50% (Gy)	2.8 ± 0.2	3.4 ± 0.6	2.6 ± 0.3	2.6 ± 0.2	a,d,e
	V6Gy (%)	12.9 ± 2.4	14.1 ± 6.3	5.0 ± 4.1	4.8 ± 2.8	b,c,d,e
L Optic Nerve	Mean (Gy)	18.9 ± 5.3	15.6 ± 7.4	9.4 ± 5.4	9.9 ± 6.1	a,b,c,d,e
	D1% (Gy)	36.2 ± 15.8	32.7 ± 17.9	28.7 ± 19.9	28.8 ± 19.4	b,c,d,e
	D10% (Gy)	30.6 ± 13.7	25.8 ± 14.5	18.9 ± 13.8	19.3 ± 14.3	a,b,c,d,e
	D50% (Gy)	16.6 ± 3.7	13.6 ± 6.1	6.8 ± 3.2	7.6 ± 4.2	b,c,d,e
R Optic Nerve	Mean (Gy)	16.5 ± 3.5	15.3 ± 5.0	7.6 ± 3.1	8.2 ± 3.5	b,c,d,e
	D1% (Gy)	36.0 ± 13.6	35.1 ± 14.1	28.2 ± 18.0	28.0 ± 17.1	b,c,d,e
	D10% (Gy)	27.3 ± 11.6	25.3 ± 10.2	16.4 ± 10.6	16.7 ± 10.1	b,c,d,e
	D50% (Gy)	14.4 ± 4.9	13.2 ± 4.3	5.1 ± 1.5	5.9 ± 2.1	b,c,d,e
Lens	D1% (Gy)	5.7 ± 0.8	9.0 ± 1.0	3.8 ± 1.0	3.8 ± 0.7	a,b,c,d,e

p < 0.05: comparisons significant at a level of 0.05 or less; CI95%: Conformity index for 95% isodoses; EI% percentage of brain receiving more than prescription dose; ID: Integral dose (10⁵ × Gy × cm³).

Comparisons: a: HT2 vs. RA2_1; b: HT2 vs. RA2_2; c: HT2 vs. RA2_3; d: RA2_1 vs. RA2_2; e: RA2_1 vs. RA2_3; f: RA2_2 vs. RA2_3; i.e. RA2_1 vs. RA2_3 is RA plan with 2mm PTV, 1 co-planar arc compared to RA plan with 2mm PTV and 3 non-coplanar fields.

coverage. D95 was greater than 50 Gy for all techniques with both the 2 and 10 mm PTV margins, and all GTV and PTV dose metrics were similar. Dose homogeneity (D1 – D99) was excellent among all the techniques; conformity indices for the RA plans were marginally better than for the HT plans, 1.3–1.4 versus 1.5–1.6, respectively (Tables 1 and 2).

DISCUSSION

Contouring of the hippocampi using CT-based anatomical landmarks allowed these structures to be designated as avoidance volumes in HT and volumetric arc planning, with consequent reduction in hippocampus dose. Barani et al. have postulated the dose tolerance of the neural

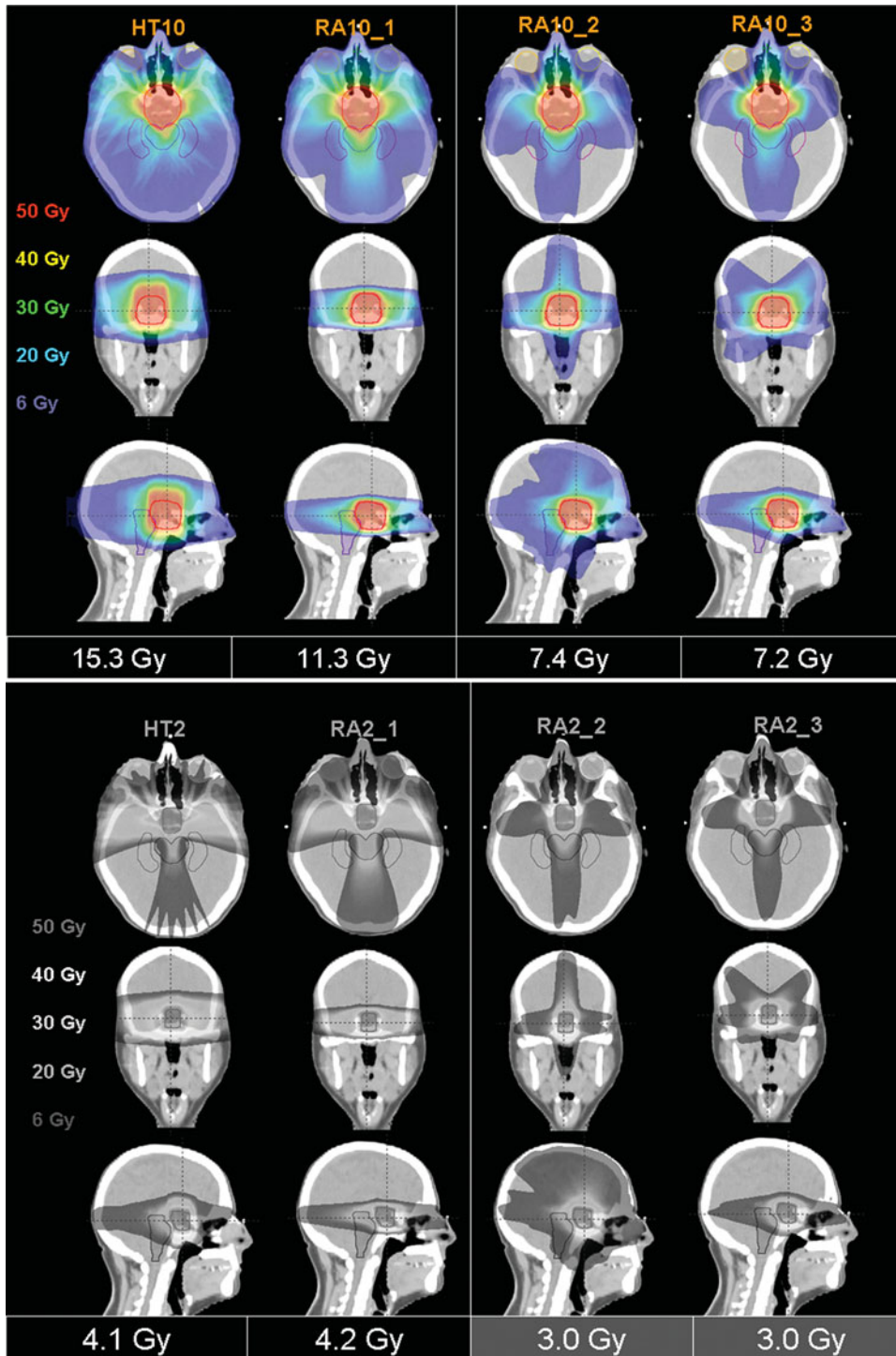


Figure 2. (a) Dose distributions in axial, coronal, and sagittal views for the radiation delivery plans with a 10 mm GTV to PTV margin for (on left): HT, co-planar volumetric arc, (on right) non-coplanar 2 orthogonal volumetric arc, and non-coplanar 3 arc techniques. Mean dose to the hippocampi are indicated below each technique. (b) Dose distributions in axial, coronal, and sagittal views for the radiation delivery plans a 2 mm GTV to PTV margin for (on left): HT, co-planar volumetric arc, (on right) non-coplanar 2 orthogonal volumetric arc, and non-coplanar 3 arc techniques. Mean dose to the hippocampi are indicated below each technique.

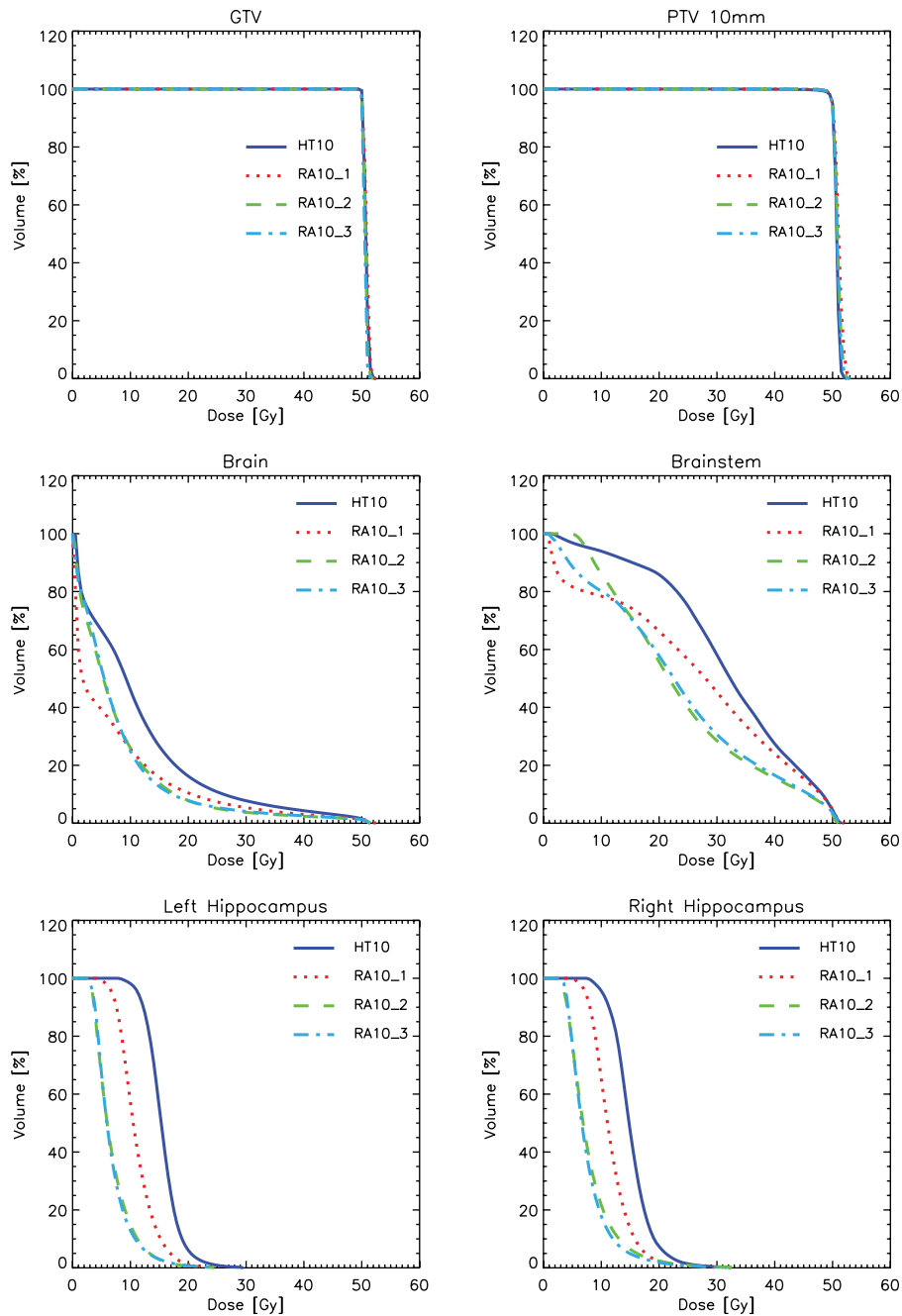


Figure 3. (a) Composite dose–volume histograms of the PTV and organs at risk for plans with a 10 mm GTV to PTV margin for helical tomotherapy (HT10; blue solid), co-planar volumetric arc (RA_1; red dots), non-coplanar 2 arc (RA_2; green dash), and non-coplanar 3 arc techniques (RA_3; blue dash). (b) Composite dose–volume histograms of the PTV and organs at risk for a 2 mm GTV to PTV margins for helical tomotherapy (HT10; blue solid), co-planar volumetric arc (RA_1; red dots), non-coplanar 2 arc (RA_2; green dash), and non-coplanar 3 arc techniques (RA_3; blue dash).

stem cells compartments, including the hippocampus, to be in the range of 10–20 Gy^{9,10} and this corresponds to clinical observations of a threshold for neurocognitive side effects and

MRI changes when doses exceed 18–20 Gy.¹⁹ Gutiérrez et al. in comparison set objectives of keeping the dose to the entire hippocampi less than 6 Gy, recognising the

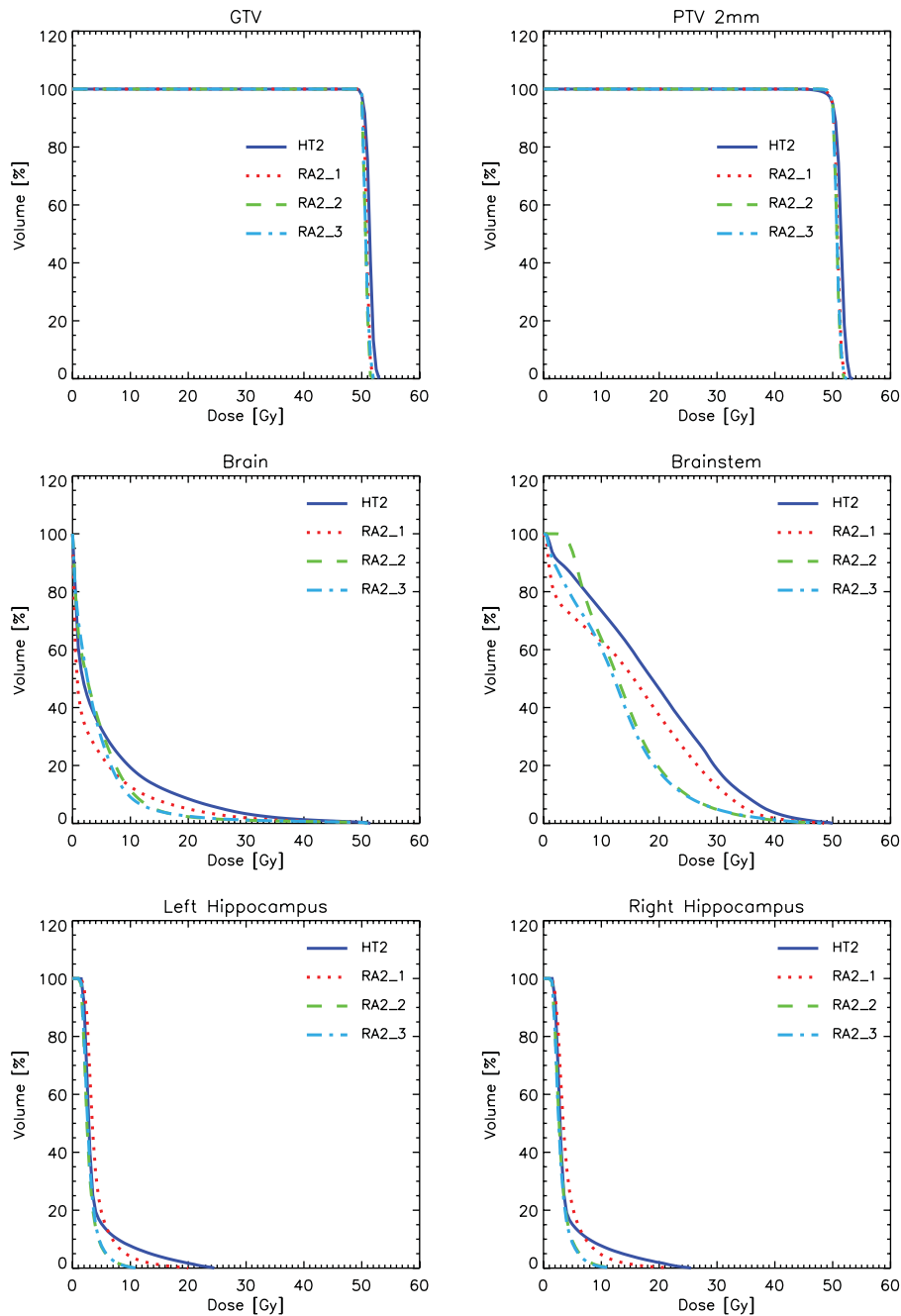


Figure 3. (Continued)

radiosensitivity of stem cell populations.¹¹ In our planning study, the combination of a tight PTV margin and intensity modulated arc delivery (via coplanar or non-coplanar techniques) allowed a reduction of hippocampus dose to a mean dose of 3–4 Gy, while maintaining

PTV coverage and respecting other OAR tolerance doses, meeting the most stringent dose objectives above.¹¹ Given the fact that our hippocampal volumes were generous (due to contouring on CT vs. MRI), sparing with MRI defined hippocampal volumes (or ideally

imaging defined stem cell sub-compartments) could be anticipated to be even more profound. In comparison, a standard, coplanar three field pituitary plan or non-hippocampus sparing coplanar intensity modulated arc delivery might be expected to deliver doses of 20–25 Gy to the hippocampi (Figure 1), in excess of the doses postulated to result in stem cell loss and neurocognitive changes.^{12,16,19}

The coplanar nature of the skull base and hippocampus creates challenges in sparing these structures without increasing brainstem or eye dose due to the limited numbers of in plane “corridors” to deliver dose to central tumours while simultaneously limiting dose to the surrounding OAR. This limitation applies to both HT and co-planar IMRT delivery techniques and has been noted by other authors.²³ In our comparisons, the use of tighter PTV margins was of greater importance than non-coplanar delivery or co-planar technique with respect to sparing of both hippocampi and other OAR. The CTV margin can be minimised through improved GTV and CTV definition by accurate multi-modality imaging and co-registration for contouring, and the PTV margin can be minimised through accurate localisation for treatment using non-invasive stereotactic image guidance techniques such as optical or on-board CT guidance.⁵ In situations where the PTV is in close proximity to multiple OAR due to larger margins or target anatomy, our comparisons suggest non-coplanar arcs may confer an advantage over co-planar delivery. Others authors have reported improved results with non-coplanar versus coplanar radiation delivery for base of skull tumours.²³ A potential disadvantage of non-coplanar arc delivery is the possibility of exit of arcs through structures such as the lungs, thyroid and other soft tissues outside of the calvarium (depending on the orientation of the arcs). Thus a strategy of optimising PTV margins combined with coplanar delivery might be the most prudent if considering dose reduction to extracranial structures.

Given the importance of planning margins, improved delineation of target and OAR volumes could also improve margin design to facilitate OAR sparing. For instance, the pres-

ence of neuron progenitor cells in the human hippocampus and subventricular zone has been confirmed through in vivo imaging with ¹H-MRS.²⁴ This finding suggests that in the future, non-invasive delineation of stem cell populations might be incorporated into the planning process for conformal avoidance, thus sparing stem cells and allowing for regeneration and repair of surrounding neural tissue. As a simpler approach to spare the subventricular neural stem cell zone along the lateral aspect of the lateral ventricles without functional imaging techniques, Barani et al. recommend designating an avoidance area within a 5 mm lateral expansion of the lateral ventricles to optimise neural stem cell preservation during radiation delivery.^{9,10} The hippocampi are paired bilateral structures, of which the left hippocampus is generally dominant for memory in right-handed individuals. Selective sparing of the dominant hippocampus and associated neural stem cell region, or the hippocampus contralateral to the tumour volume for more lateralised tumours, might also facilitate neural stem cell-sparing radiation plans.

Ultimately, the efficacy of stem cell sparing techniques needs to be confirmed through correlation between dosimetry and relevant neurocognitive outcomes in prospectively treated patients. Future considerations for ongoing research in this area could include a magnetic resonance–spectroscopy study of patients previously treated with radiation for CNS tumours. Spectral changes in hippocampus could be quantified and correlated with radiation dose to hippocampus dose received. Prospective functional imaging studies could evaluate the degree of activity preserved with hippocampus sparing radiotherapy techniques. Such morphologic and spectroscopic changes have been described for patients with neurodegenerative disease such as Alzheimer’s^{25–27} and may be a complement to traditional neurocognitive testing, particularly as a potential early biomarker of injury.

CONCLUSIONS

Patients with base of brain tumours represent a patient population with long-life expectancy

after treatment for malignancy, and stand to gain significant benefit from reducing late neurocognitive sequelae of radiation treatments. Hippocampus contouring and specification as an avoidance structure in helical or volumetric arc techniques can achieve significant reduction in dose to the hippocampi. Our comparisons suggest interventions to minimise GTV to PTV margins will have a more profound influence on multiple OAR sparing than the choice of intensity modulated arc delivery technique. Prospective studies with larger numbers of patients treated with a wider variety of base of skull tumours and including neurocognitive endpoints would help define the potential clinical benefits of these hippocampal sparing techniques.

Conflict of interest

Dr. L. Cozzi acts as Scientific Advisor to Varian Medical Systems and is Head of Research and Technological Development to Oncology Institute of Southern Switzerland, IOSI, Bellinzona.

References

- Schultheiss TE, Kun LE, Ang KK, Stephens LC. Radiation response of the central nervous system. *Int J Radiat Oncol Biol Phys* 1995; 31: 1093–1112.
- Byrne TN. Cognitive sequelae of brain tumor treatment. *Curr Opin Neurol* 2005; 18: 662–666.
- McCord MW, Buatti JM, Fennell EM, Mendenhall WM, Marcus RB Jr, Rhoton AL, Grant MB, Friedman WA. Radiotherapy for pituitary adenoma: long-term outcome and sequelae. *Int J Radiat Oncol Biol Phys* 1997; 39: 437–444.
- Noad R, Narayanan KR, Howlett T, Lincoln NB, Page RC. Evaluation of the effect of radiotherapy for pituitary tumours on cognitive function and quality of life. *Clin Oncol (R Coll Radiol)* 2004; 16: 233–237.
- Bauman G, Wong E, McDermott M. Fractionated radiotherapy techniques. *Neurosurg Clin N Am* 2006; 17: 99–110, v.
- Monje ML, Mizumatsu S, Fike JR, Palmer TD. Irradiation induces neural precursor-cell dysfunction. *Nat Med* 2002; 8: 955–962.
- Eriksson PS, Perfilieva E, Björk-Eriksson T, Alborn AM, Nordborg C, Peterson DA, Gage FH. Neurogenesis in the adult human hippocampus. *Nat Med* 1998; 4: 1313–1317.
- Hellström NA, Björk-Eriksson T, Blomgren K, Kuhn HG. Differential recovery of neural stem cells in the subventricular zone and dentate gyrus after ionizing radiation. *Stem Cells* 2009; 27: 634–641.
- Barani IJ, Benedict SH, Lin PS. Neural stem cells: implications for the conventional radiotherapy of central nervous system malignancies. *Int J Radiat Oncol Biol Phys* 2007; 68: 324–333.
- Barani IJ, Cuttino LW, Benedict SH, et al. Neural stem cell-preserving external-beam radiotherapy of central nervous system malignancies. *Int J Radiat Oncol Biol Phys* 2007; 68: 978–985.
- Gutiérrez AN, Westerly DC, Tomé WA, Jaradat HA, Mackie TR, Bentzen SM, Khuntia D, Mehta MP. Whole brain radiotherapy with hippocampal avoidance and simultaneously integrated brain metastases boost: a planning study. *Int J Radiat Oncol Biol Phys* 2007; 69: 589–597.
- Sohn JW, Dalzell JG, Suh JH, Tefft M, Schell MC. Dose-volume histogram analysis of techniques for irradiating pituitary adenomas. *Int J Radiat Oncol Biol Phys* 1995; 32: 831–837.
- Cozzi L, Clivio A, Bauman G, Cora S, Nicolini G, Pellegrini R, Vanetti E, Yartsev S, Fogliata A. Comparison of advanced irradiation techniques with photons for benign intracranial tumours. *Radiother Oncol* 2006; 80: 268–273.
- Killiany RJ, Hyman BT, Gomez-Isla T, Moss MB, Kikinis R, Jolesz F, Tanzi R, Jones K, Albert MS. MRI measures of entorhinal cortex vs hippocampus in preclinical AD. *Neurology* 2002; 58: 1188–1196.
- Shepard DM, Olivera GH, Reckwerdt PJ, Mackie TR. Iterative approaches to dose optimization in tomotherapy. *Phys Med Biol* 2000; 45: 69–90.
- Yartsev S, Kron T, Cozzi L, Fogliata A, Bauman G. Tomotherapy planning of small brain tumours. *Radiother Oncol* 2005; 74: 49–52.
- Cozzi L, Dinshaw KA, Shrivastava SK, Mahantshetty U, Engineer R, Deshpande DD, Jamema SV, Vanetti E, Clivio A, Nicolini G, Fogliata A. A treatment planning study comparing volumetric arc modulation with RapidArc and fixed field IMRT for cervix uteri radiotherapy. *Radiother Oncol* 2008; 89: 180–191.
- Fogliata A, Clivio A, Nicolini G, Vanetti E, Cozzi L. Intensity modulation with photons for benign intracranial tumours: a planning comparison of volumetric single arc, helical arc and fixed gantry techniques. *Radiother Oncol* 2008; 89: 254–262.
- Steen RG, Spence D, Wu S, Xiong X, Kun LE, Merchant TE. Effect of therapeutic ionizing radiation on the human brain. *Ann Neurol* 2001; 50: 787–795.
- Du AT, Schuff N, Amend D, Laakso MP, Hsu YY, Jagust WJ, Yaffe K, Kramer JH, Reed B, Norman D, Chui HC, Weiner MW. Magnetic resonance imaging of the entorhinal cortex and hippocampus in mild cognitive impairment and Alzheimer's disease. *J Neurol Neurosurg Psychiatr* 2001; 71: 441–447.
- Gladwish A, Kron T, McNiven A, Bauman G, Van Dyk J. Asymmetric fan beams (AFB) for improvement of the

- craniocaudal dose distribution in helical tomotherapy delivery. *Med Phys* 2004; 31: 2443–2448.
22. Mackie TR, Balog J, Ruchala K, Shepard D, Aldridge S, Fitchard E, Reckwerdt P, Olivera G, McNutt T, Mehta M. Tomotherapy. *Semin Radiat Oncol* 1999; 9: 108–117.
 23. Soisson ET, Tomé WA, Richards GM, Mehta MP. Comparison of linac based fractionated stereotactic radiotherapy and tomotherapy treatment plans for skull-base tumors. *Radiother Oncol* 2006; 78: 313–321.
 24. Manganas LN, Zhang X, Li Y, Hazel RD, Smith SD, Wagshul ME, Henn F, Benveniste H, Djuric PM, Enikolopov G, Maletic-Savatic M. Magnetic resonance spectroscopy identifies neural progenitor cells in the live human brain. *Science* 2007; 318: 980–985.
 25. Frederick BD, Lyoo IK, Satlin A, Ahn KH, Kim MJ, Yurgelun-Todd DA, Cohen BM, Renshaw PF. In vivo proton magnetic resonance spectroscopy of the temporal lobe in Alzheimer's disease. *Prog Neuropsychopharmacol Biol Psychiatry* 2004; 28: 1313–1322.
 26. Ramani A, Jensen JH, Helpem JA. Quantitative MR imaging in Alzheimer disease. *Radiology* 2006; 241: 26–44.
 27. Jack CR Jr, Petersen RC, Xu YC, O'Brien PC, Smith GE, Ivnik RJ, Boeve BF, Waring SC, Tangalos EG, Kokmen E. Prediction of AD with MRI-based hippocampal volume in mild cognitive impairment. *Neurology* 1999; 52: 1397–1403.